

benzaldehyde, 14.6; 2-acetoxy-4-methylanisole, 16.8; 3-acetoxy-4-methylanisole, 20.0; *p*-methoxybenzyl acetate, 28.0; unknown peak I (molecular weight 194), 30.5; and unknown peak II (molecular weight 194), 38.2.

Acknowledgment. The author gratefully acknowledges the financial support of the Swedish Natural Science Research Council.

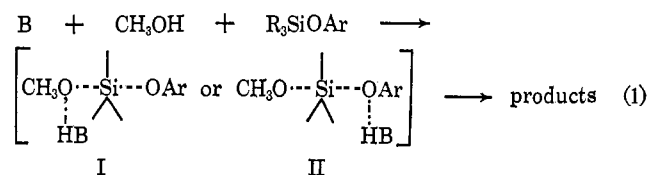
The Transition State for Base-Catalyzed Cleavage of the Silicon–Oxygen Bond¹

Richard L. Schowen and Kenyon S. Latham, Jr.

Contribution from the Department of Chemistry, University of Kansas, Lawrence, Kansas 66044. Received March 20, 1967

Abstract: Substituent correlations and solvent isotope effects have been examined for the general base catalyzed methanolysis of aryloxytriphenylsilanes, previously shown to follow a protolytic mechanism. The solvent isotope effects for *p*-chlorophenoxytriphenylsilane are $k_H/k_D = 1.25 \pm 0.06$ (acetate ion catalysis) and 1.35 ± 0.06 (methoxide ion catalysis), consistent with "solvation-rule" behavior. Curvature in the free-energy relations for leaving-group structural variation is analyzed and is tentatively interpreted in terms of π bonding of the leaving group to silicon in the activated complex or of a change in mechanism with substituent.

Our earlier observation¹ that the methanolysis of phenoxytriphenylsilane is subject to general base catalysis by phenoxide ion, leading to the conclusion that the reaction follows a protolytic pathway (eq 1), further substantiates a general resemblance of these reactions to the cleavage of carboxylic and phosphate esters. We have therefore undertaken a more detailed characterization of the transition state for base-catalyzed solvolysis of silicon–oxygen compounds, by use of isotope and substituent effects.



Results

Observed rate constants for methanolysis of five aryloxytriphenylsilanes in acetic acid–acetate ion buffers in methanol and methanol-*d*₁ (CH₃OD) and in phenol–phenoxide ion buffers in methanol are given in Table I. The results may be summarized by the kinetic law of eq 2, where S represents the substrate organosilicon compound and the summation is over all bases, B_{*i*}, in the solution. The values of the catalytic constants of eq 2 are shown in Table II. From corresponding rate constants in methanol and methanol-*d*₁, the isotope effects for methanolysis of *p*-chlorophenoxytriphenylsilane, catalyzed by acetate and methoxide ions, can be calculated.

(1) Catalysis in Organosilicon Chemistry. II. For part I, see R. L. Schowen and K. S. Latham, Jr., *J. Am. Chem. Soc.*, **88**, 3795 (1966). For further details, see K. S. Latham, Jr., Ph.D. Thesis, University of Kansas, Oct 1966. This work was supported by the National Science Foundation under Research Grant No. GP 3539 and by the National Institutes of Health under Research Grant No. GM 12477-02 and was carried out in part at the Computation Center of the University of Kansas.

$$(k_H/k_D)_{\text{CH}_3\text{CO}_2^-} = 1.25 \pm 0.06$$

$$(k_H/k_D)_{\text{CH}_3\text{O}^-} = 1.35 \pm 0.06$$

$$v = [\text{S}] \left\{ k_0 + \sum_i k_i [\text{B}_i] \right\} \quad (2)$$

Discussion

Solvent Isotope Effects. The activated complex drawn in eq 1 for the reaction under study depicts a proton undergoing transfer from or to the catalyst. If such a transfer were part of the primary activation process, so that the proton would be in an unstable potential at the activated complex, a primary isotope effect of about 7.8, corresponding to the Brønsted β value¹ of about 0.7, would have been expected.² The observed isotope effects are much smaller than the predicted ones, and it therefore appears likely that the proton is not in an unstable potential at the activated complex; the BH moiety is presumably stabilizing the activated complex by a hydrogen-bonding interaction, as postulated by Swain and his co-workers³ for other examples of general catalysis in protic solvents. The methanolysis of aryloxysilanes appears to conform to the "solvation rule" classification³ as do carbonyl derivative reactions in which the leaving group is an oxyanion.²

These isotope effects present an interesting contrast to the striking observation of Menger⁴ that methoxide ion attack on *p*-nitrophenyl acetate proceeds 2.6 times more rapidly in methanol-*d* than in methanol at -78° . If a completely exponential temperature dependence with unit preexponential factor is assumed ($k_H/k_D = \exp(-a/T)$) the inverse isotope effect is still 1.9 at 25° , equal to the effect reported by Menger⁴ for methoxide attack on phenyl benzoate at 25° . The regular effects

(2) The primary isotope effect prediction is made with the aid of Figure 1 of R. L. Schowen, H. Jayaraman, L. Kershner, and G. W. Zuorick, *J. Am. Chem. Soc.*, **88**, 4008 (1966).

(3) C. G. Swain, D. A. Kuhn, and R. L. Schowen, *ibid.*, **87**, 1553 (1965).

(4) F. M. Menger, *ibid.*, **88**, 5356 (1966).

Table I.^a Observed Rate Constants for Methanolysis of $\text{XC}_6\text{H}_4\text{OSi}(\text{C}_6\text{H}_5)_3$ in Methanolic Buffer Solutions at $27.4 \pm 0.1^\circ$

X	[B]/[BH]	[B], M	$10^3 k_{\text{obsd}}^b$	X	[B]/[BH]	[B], M	$10^3 k_{\text{obsd}}^b$		
Acetate-Acetic Acid Buffers, Methanol- <i>h</i>									
<i>p</i> -CH ₃ O	15.0	0.0750	1.80	<i>m</i> -CF ₃	5.0	0.0375	5.69		
	15.0	0.1150	1.81		5.0	0.0750	7.33		
	15.0	0.1500	1.94		5.0	0.1125	8.87		
	12.0	0.1200	1.61		4.76	0.0500	47.2		
	10.7	0.0300	1.23		4.76	0.0750	63.2		
	10.7	0.0600	1.26		4.76	0.1000	73.4		
	10.7	0.0900	1.34		3.46	0.0500	38.9		
	10.7	0.1200	1.40		3.46	0.0750	52.5		
	10.0	0.0500	1.18		3.46	0.1000	66.3		
	10.0	0.1000	1.20		2.68	0.0500	33.3		
	10.0	0.1500	1.30		2.68	0.0750	48.2		
	5.0	0.0500	0.69		2.68	0.1000	61.2		
	5.0	0.0600	0.77		Phenoxide-Phenol Buffers, Methanol- <i>h</i>				
	5.0	0.0900	0.83		<i>p</i> -CH ₃ O	0.100	0.0005	21.2 ^b	
	5.0	0.1200	0.84			0.100	0.0010	19.2	
<i>p</i> -CH ₃	15.0	0.0500	1.80	0.100		0.0015	26.2		
	15.0	0.1000	1.83	0.050	0.0005	6.11			
	15.0	0.1500	1.98	0.050	0.0010	7.63			
	10.0	0.0500	1.34	0.050	0.0015	8.06			
	10.0	0.1000	1.44	<i>p</i> -CH ₃	0.050	0.0005	5.39		
	10.0	0.1500	1.53		0.050	0.0010	6.09		
	5.0	0.0500	0.71		0.050	0.0015	6.51		
H	5.0	0.1000	0.83	H	0.050	0.0005	10.0		
	5.0	0.1500	0.88		0.050	0.0010	11.2		
	H	15.0	0.0500		2.88	0.050	0.0020	15.5	
		15.0	0.1000		3.18	<i>p</i> -Cl	0.050	0.0001	21.6
		15.0	0.1500		3.37		0.050	0.0003	34.3
10.0	0.0500	2.03	0.050	0.0005	40.5				
<i>p</i> -Cl	10.0	0.1000	2.13	Acetate-Acetic Acid Buffers, Methanol- <i>d</i>					
	10.0	0.1500	2.42	$10^3[\text{CH}_3\text{O}^-],$					
	<i>p</i> -Cl	8.0	0.0375	7.22	M				
		8.0	0.0750	8.92	<i>p</i> -Cl	46.8	0.0300	1.95 ^b	
		8.0	0.1125	10.26		46.8	0.0750	3.25	
7.0		0.0375	6.80	46.8		0.1200	4.13		
7.0		0.0750	8.49	62.4		0.0750	4.99		
7.0	0.1125	10.03							

^a Ionic strength 0.1500 M (adjusted by addition of LiClO₄) in all runs. Standard deviations of rate constants are $\pm 1.5\%$ (acetate buffers in CH₃OD), $\pm 2.5\%$ (acetate buffers in CH₃OH), and $\pm 5\%$ (phenoxide buffers in CH₃OH). ^b Rate constants are tabulated in min⁻¹ for acetate buffers in CH₃OH and CH₃OD and in sec⁻¹ for phenoxide buffers in CH₃OH.

Table II.^a Catalytic Constants for Methanolysis of $\text{XC}_6\text{H}_4\text{OSi}(\text{C}_6\text{H}_5)_3$ in Methanol-*h* and Methanol-*d* at $27.4 \pm 0.1^\circ$ ($\mu = 0.1500$ M)

X	Solvent	$k_B, M^{-1} \text{sec}^{-1}$			$10^3 k_0,^b$ sec ⁻¹
		CH ₃ CO ₂ ⁻	C ₆ H ₅ O ⁻	CH ₃ O ⁻	
<i>p</i> -CH ₃ O	CH ₃ OH	2.62×10^{-5}	1.62	45.7	0.3
<i>p</i> -CH ₃	CH ₃ OH	3.98×10^{-5}	1.15	50.0	0.2
H	CH ₃ OH	6.57×10^{-5}	3.61	94.0	-0.1
<i>p</i> -Cl	CH ₃ OH	71.3×10^{-5}	49.4	250	3.0
	CH ₃ OD	57.2×10^{-5}		185	
<i>m</i> -CF ₃	CH ₃ OH	893×10^{-5}		3313	

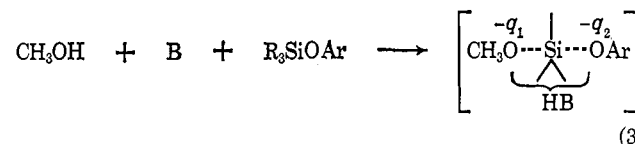
^a The catalyst constants are defined by eq 2. ^b These small terms presumably originate in experimental error, catalysis by trace impurities, or catalysis by solvent ("uncatalyzed" solvolysis).

observed in the organosilicon reaction are in complete consistency with the fact that small residual isotope effects are usually found after correction of "solvation rule" isotope effects for secondary contributions in aqueous solution.³ These effects presumably arise from a combination of solvation-change isotope effects⁵ and ones due to vibrational shifts on

(5) C. G. Swain and R. F. W. Bader, *Tetrahedron*, **10**, 182 (1960); C. G. Swain, R. F. W. Bader, and E. R. Thornton, *ibid.*, **10**, 200 (1960); C. G. Swain and E. R. Thornton, *J. Am. Chem. Soc.*, **83**, 3884, 3890 (1961).

formation of the strong hydrogen bonds of the catalytic site.⁶

Substituent Effects on Free Energy. The activation process under study here (eq 3) may be compared with the model process of eq 4 in order to assess the elec-



tronic conditions in the leaving group zone of the activated complex. The substituent effects on the free energy of activation ($\delta_x \Delta G^*$) and on the free energy of neutralization of the phenols' ($\delta_x \Delta G^\circ$) would be expected to yield a relation (eq 5) the slope, m , of which should approximate the magnitude of q_2 (eq 3), the

$$\delta_x \Delta G^* = m \delta_x \Delta G^\circ \quad (5)$$

charge on the activated complex leaving group.⁸

(6) C. A. Bunton and V. J. Shiner, *ibid.*, **83**, 42, 3207, 3214 (1961).

(7) These quantities were measured for methanol solution in this laboratory, using the spectrophotometric method given in the Experimental Section.

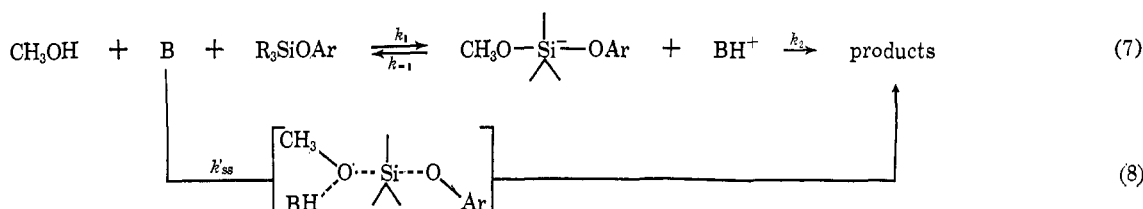
(8) J. E. Leffler and E. Grunwald, "Rates and Equilibria of Organic

It has been a frequent experience⁹ that such simple interpretations of free energy correlation slopes (*e.g.*, the particularly straightforward interpretations of Brønsted parameters^{3,8}) are difficult to reconcile with enthalpy-entropy data, when these are available. For example, the resonance and inductive effects usually attributed to remote substituents should both contribute to the observed enthalpies, whereas the actual situation in solution reactions is often that both enthalpies and entropies vary, sometimes in a complicated way.^{10,11} Hepler's brilliant treatment¹² of phenol ionization resolves this difficulty for aqueous solution. He argues that (a) observed substituent effects on enthalpies are sums of internal energy contributions ($\delta\Delta H_{\text{int}}$, containing resonance and inductive effects) and of external contributions ($\delta\Delta H_{\text{ext}}$, chiefly due to solvation phenomena), as in eq 6; (b) no entropy changes are associated with $\delta\Delta H_{\text{int}}$, but¹³ $\delta\Delta H_{\text{ext}} = 280\delta\Delta S_{\text{ext}}$ so that the free energy effect is given by eq 6b (since $\delta\Delta S_{\text{ext}} \approx \delta\Delta S$). The approximate equality of free

$$\delta\Delta H = \delta\Delta H_{\text{int}} + \delta\Delta H_{\text{ext}} \quad (6a)$$

$$\delta\Delta G = \delta\Delta H_{\text{int}} + (280 - T)\delta\Delta S \approx \delta\Delta H_{\text{int}} \quad (6b)$$

energy effects and internal effects arises at temperatures near 280°K and seems to underlie a great fraction of linear free energy relations in aqueous media.^{14,15} In addition, it has been found possible to understand the substituent effect on the activation process for methoxide-catalyzed methanolysis of aryl methyl carbonates¹⁶ and aryl acetates¹⁷ by use of Hepler's ideas, with adoption of 320°K for the compensation temperature appropriate to solvation interaction in methanol. We therefore are reasonably confident of the interpreta-



tion of the present free energy data in internal energy terms.

Figure 1 shows a plot of $\delta_x\Delta G^*_B$ for methanolysis of aryloxytriphenylsilanes by three catalyzing bases, acetate ion, phenoxide ion, and methoxide ion, *vs.* $\delta_x\Delta G^\circ$ for neutralization of phenols under the same conditions (data of Table III). The positive sign of m (eq 5) is expected (activated complex stabilization by

Reactions," John Wiley and Sons, Inc., New York, N. Y., 1962, pp 156-161, and following. See also the discussion of the δ operator by these authors on p 26 of this book.

(9) *E.g.*, see P. G. Ashworth, "Catalysis and Inhibition of Chemical Reactions," Butterworth and Co. (Publishers) Ltd., London, 1963, Chapter I.

(10) Reference 8, Chapter 9.

(11) R. W. Taft, Jr., in "Steric Effects in Organic Chemistry," M. S. Newman, Ed., John Wiley and Sons, Inc., New York, N. Y., 1956.

(12) L. G. Hepler, *J. Am. Chem. Soc.*, **85**, 3089 (1963).

(13) The value of 280°K for the compensation temperature in water was taken from studies by R. F. Brown, *J. Org. Chem.*, **27**, 3015 (1962).

(14) E. M. Arnett and J. J. Burke, *J. Am. Chem. Soc.*, **88**, 4308 (1966).

(15) R. L. Schowen, *J. Pharm. Sci.*, in press.

(16) R. L. Schowen, C. G. Mitton, and J. Shapley, submitted for publication. See Abstracts of the 152nd National Meeting of the American Chemical Society, New York, N. Y., Sept 1966, Paper S139.

(17) C. G. Mitton and Michael Gresser, unpublished results.

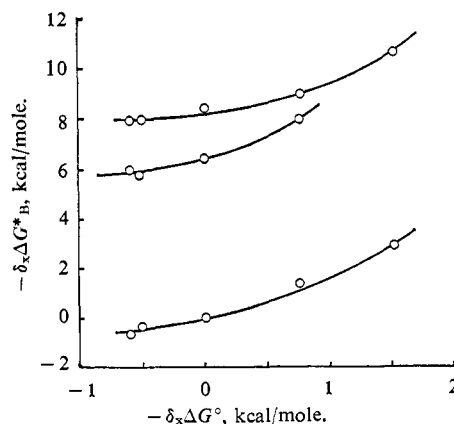


Figure 1. Substituent effect on the free energy of activation for methanolysis of aryloxytriphenylsilanes catalyzed by methoxide ion (top line), phenoxide ion (middle line), and acetate ion (bottom line) *vs.* substituent effect on the free energy of ionization of the corresponding arylol in methanol under the same conditions.

electron withdrawal), but the curvature is surprising.¹⁸ Curvature of free energy relations for other reactions has been attributed to (a) a gross change in reaction mechanism with reactant structural variation,¹⁹ (b) change in the rate-determining step of a multistep sequence as a function of reactant structure,²⁰ and (c) gradual variation in activated complex structure with reactant structure.²¹ We shall consider these possibilities in turn.

Change in Mechanism. Two mechanisms are reasonably conceivable for this reaction:¹ a two-step, "Si-5" mechanism²² (eq 7) and a concerted displacement process (eq 8). For the two-step mechanism, the k_1

step is probably¹ rate determining since ArO^- is a better leaving group¹⁶ than CH_3O^- ; more complex possibilities are discussed below. If the kinetics of a series of competing reactions are the same, the most general expression (eq 9) for the observed rate constant (k_o) is a sum of the rate constants, k_i , for the competing

$$k_o = \sum k_i \quad (9)$$

mechanisms. Converting to free energies and applying the substituent variation operator (δ_x), defining f_i (eq 12) as the fraction of the total reaction proceeding by

$$\Delta G^*_0 = -RT \ln \sum_i \exp(-\Delta G^*_i/RT) \quad (10)$$

(18) The curvature is well outside experimental error (see Table III). The same kind of curvature is also readily apparent on examination of the Hammett plots of E. Åkerman (*Acta Chem. Scand.*, **10**, 298 (1956); **11**, 373 (1957)) for the more complex reaction of basic aqueous ethanol with aryloxysilanes.

(19) Y. Okamoto and H. C. Brown, *J. Org. Chem.*, **22**, 485 (1957).

(20) W. P. Jencks, *Progr. Phys. Org. Chem.*, **2**, 63 (1964); J. F. Kirsch and W. P. Jencks, *J. Am. Chem. Soc.*, **86**, 833, 837 (1964).

(21) (a) C. G. Swain and W. P. Langsdorf, *ibid.*, **73**, 2813 (1951); (b) C. G. Swain and R. L. Schowen, *J. Org. Chem.*, **30**, 615 (1965).

(22) L. H. Sommer, "Stereochemistry, Mechanism and Silicon," McGraw-Hill Book Co., Inc., New York, N. Y., 1965, p 131.

Table III.^{a,b} Substituent Effects on Free Energies of Activation for Catalyzed Methanolysis of $\text{XC}_6\text{H}_5\text{OSi}(\text{C}_6\text{H}_5)_3$ ($\delta_x\Delta G^*_B$) and on Dissociation of $\text{XC}_6\text{H}_4\text{OH}$ in Methanol ($\delta_x\Delta G^\circ$)

X	$\delta_x\Delta G^*_\text{C}_6\text{H}_5\text{CO}_2^-$	$\delta_x\Delta G^*_\text{C}_6\text{H}_5\text{O}^-$	$\delta_x\Delta G^*_\text{C}_6\text{H}_5\text{O}^-$	$\delta_x\Delta G^\circ$
<i>p</i> -CH ₃ O	+0.54	-6.01	-7.98	0.60
<i>p</i> -CH ₃	+0.29	-5.80	-8.05	0.51
H	0.0	-6.47	-8.43	0.0
<i>p</i> -Cl	-1.40	-8.04	-9.00	-0.77
<i>m</i> -CF ₃	-2.90		-10.52	-1.52

^a Rate data are for $27.4 \pm 0.1^\circ$, equilibrium data for $25.0 \pm 0.1^\circ$. All numbers are in kcal/mole; errors are about ± 0.03 kcal/mole. ^b Rate data are relative to $\Delta G^*_\text{C}_6\text{H}_5\text{CO}_2^-$, $\text{C}_6\text{H}_5\text{OSi}(\text{C}_6\text{H}_5)_3$; equilibrium data are relative to ΔG° , $\text{C}_6\text{H}_5\text{OH}$.

$$\delta_x\Delta G^*_0 = \sum_i \delta_x\Delta G^*_i \exp(-\Delta G^*_i/RT) / \sum_i \exp(\Delta G^*_i/RT) \quad (11)$$

$$f_i \equiv \exp(-\Delta G^*_i/RT) / \sum_i \exp(-\Delta G^*_i/RT) \quad (12)$$

$$\delta_x\Delta G_0 = \sum_i f_i \delta_x\Delta G_i \quad (13)$$

$$\delta_x\Delta G^*_i = m_i \delta_x\Delta G^\circ \quad (14)$$

$$\delta_x\Delta G^*_0 = \left(\sum_i f_i m_i \right) \delta_x\Delta G^\circ = m_0 \delta_x\Delta G^\circ \quad (15)$$

the *i*th mechanism, and assuming a rate-equilibrium correlation (eq 5) for each mechanism (eq 14), we obtain finally eq 15. This shows the observed correlation slope to be an average of the slopes appropriate to the contributing mechanisms, each weighted by the fraction of the reaction proceeding by the corresponding mechanism. Of course, the f_i should also change with reactant structure (as measured by $\delta_x\Delta G^\circ$; notice that $-\delta\Delta G^\circ$ and $-\delta_x\Delta G^*_B$ are plotted in Figure 1) and this function is obtained by application of δ_x to eq 12 and introduction of eq 14 to the result, yielding eq 16. Thus, the more positive m_i , the smaller its contribution

$$\delta_x f_i = \frac{f_i}{RT} \{m_0 - m_i\} \delta_x\Delta G_0 \quad (16)$$

to m_0 will become as $\delta_x\Delta G^\circ$ increases. In the present case, m_{ss} (for the single-step mechanism) should be larger than m_{ts} (two-step mechanism) because the Si-O bond is breaking (and negative charge is thus appearing in the leaving-group oxygen) in the single-step mechanism, whereas this bond is not breaking in the (rate-determining) activated complex, for the addition step, in the two-step reaction. Therefore at large $\delta_x\Delta G^\circ$ (poor leaving groups), $m_0 \approx m_{ts}$, while at small $\delta_x\Delta G^\circ$ (good leaving groups), $m_0 \approx m_{ss}$. Thus as $\delta_x\Delta G^\circ$ increases, m_0 should go from large values (m_{ss}) to small values (m_{ts}), as is observed.

The observed substituent effects are compatible with a change in mechanism from a single-step displacement (eq 8) with good leaving groups to a two-step displacement (eq 7) with poor leaving groups.

Change in the Rate-Determining Step. Let us now consider the possibility that the curvature in Figure 1 arises from a change in the rate-determining step of a two-step sequence (eq 7). This seems initially unlikely since any ArO^- would be expected to exceed CH_3O^- in leaving-group tendency, at least on polar grounds,¹⁶ and thus the k_1 step of eq 7 would effectively determine the rate if $k_2 > k_{-1}$. However, the hypothetical "Si-5"

intermediate may constitute a species of considerable steric compression²² and the (probably) greater bulk of the ArO^- groups might compete with the polar effect.²³ This hypothesis must therefore be discussed.

Application of the steady-state method²⁴ to eq 7 yields eq 17 for the observed rate constant. Proceeding

$$k_0 = \frac{k_1 k_2}{k_{-1} + k_2}$$

$$k_0^{-1} = k_1^{-1} + \left(\frac{k_1}{k_{-1}} k_2 \right)^{-1} \quad (17)$$

as in the last section, we obtain eq 18, where f_2 and f_{-1} , defined by eq 19, are respectively the fractions

$$\delta_x\Delta G^*_0 = f_2 \delta_x\Delta G^*_1 + f_{-1} \delta_x\Delta G^*_2 \quad (18)$$

$$f_2 = \exp(\Delta G^*_1/RT) / [\exp(\Delta G^*_1/RT) + \exp(\Delta G^*_2/RT)] \quad (19a)$$

$$f_{-1} = \exp(\Delta G^*_2/RT) / [\exp(\Delta G^*_1/RT) + \exp(\Delta G^*_2/RT)] \quad (19b)$$

$$f_2 + f_{-1} = 1 \quad (19c)$$

of the "Si-5" intermediate which proceed on to products and return to reactants; here ΔG^*_1 is the free energy of activation for conversion of reactants into the first ("addition") activated complex and ΔG^*_2 that for conversion of reactants into the second ("elimination") activated complex. Equation 18 shows the observed substituent effect to be an average of effects for formation of the two activated complexes, each weighted by the fraction of intermediate which decomposes by the *other* route. Again, assuming each of the composite processes to show a rate-equilibrium correlation, and introducing eq 19c, we have eq 20 (where m_i corresponds to ΔG^*_i).

$$\delta_x\Delta G^*_0 = (m_2 + f_2[m_1 - m_2]) \delta_x\Delta G^\circ = m_0 \delta_x\Delta G^\circ \quad (20)$$

On chemical grounds we argue that both m_1 and m_2 will be positive (since both activated complexes are electron rich relative to reactants) and that $m_2 > m_1$ since the Si-O bond is breaking in the m_2 process. Thus, from eq 20, the slope observed should be positive but should decrease as f_2 becomes larger. In the same way as above, eq 21 is found for the effect of structure on

$$\delta_x f_2 = \left[\frac{f_2(1 - f_2)}{RT} (m_1 - m_2) \right] \delta_x\Delta G^\circ \quad (21)$$

f_2 . As $\delta_x\Delta G^\circ$ increases (poorer leaving group), f_2 decreases; thus m_0 should increase as $\delta_x\Delta G^\circ$ becomes larger. This is contrary to the observations of Figure 1 and this hypothesis is therefore incompatible with the data.

Changes in Activated Complex Structure. Considerable evidence²⁵ indicates that activated complexes are more sensitive in their gross structural parameters and electron distributions than are stable molecules. Thus, although remote groups rarely exert large effects on bond lengths, angles, etc., in reactant molecules, these influences may appear in activated complexes. It

(23) Larger groups appear to be expelled with less facility than smaller groups from the tetrahedral intermediates of ester solvolysis: S. C. Hoops, Ph.D. Thesis, University of Kansas, 1967.

(24) A. A. Frost and R. G. Pearson, "Kinetics and Mechanism," 2nd ed, John Wiley and Sons, Inc., New York, N. Y., 1962.

(25) See discussions in ref 3, 21, and 26-28.

should be possible to predict the direction of such effects by using (a) the extended Hammond postulate²⁶ (EHP), (b) the Swain–Thornton reacting bond rule²⁷ (STR), and (c) the Thornton perturbation method²⁸ (TPM).

On the concerted-reaction model (eq 8), all approaches (EHP, STR, and TPM) predict that increasing electron donation (larger $\delta_x\Delta G^\circ$) will lengthen the activated complex Si \cdots OAr bond, increasing the degree of negative charge in the leaving group zone (q_2 , eq 3). If m is a measure of q_2 it would be increased, leading to a concave-downward curvature, as opposed to the concave-upward curvature observed in Figure 1. On the two-step model (eq 8), the first step should be rate determining (as explained above) and little change in m with leaving group structure is expected. Nevertheless, some change could result from variations in the position of the center of negative charge density or from differences in release of electron density onto the leaving group from oxygen $d\pi$ – $p\pi$ conjugation²⁹ with Si. Both the EHP and TPM predict that CH₃O \cdots Si will be shorter with poorer leaving groups (electron donation, larger $\delta_x\Delta G^\circ$), which should lead to a center of negative charge closer to the substituents and greater release of electron density from the Si 3d orbitals and thus a larger m at larger $\delta_x\Delta G^\circ$, again contrary to the observations.

The STR predicts, on the other hand, that electron donation will lengthen the CH₃O \cdots Si bond. This prediction is disturbing since it contains an internal contradiction for the general case of attack of various nucleophiles N on a substituted organosilicon species, RSiR'₃. If the Swain–Scott equation³⁰ (eq 22) describes the dependence of the rate on the nucleophilicity of N and the Hammett equation (eq 23) the influence

$$\log k_{RN} = S_R n_N + \log k_{RN_0} \quad (22)$$

$$\log k_{RN} = \rho_N \sigma_R + \log k_{RN_0} \quad (23)$$

of R then, as Miller³¹ has shown, a relation exists between the parameters (eq 24). The values of S_R for various substrates must be linear in σ_R and the ρ_N for various nucleophiles must be linear in n_N with the

$$(S_R - S_{R_0})/\sigma_R = (\rho_N - \rho_{N_0})/n_N = C \quad (24)$$

same slope, C . The sign of this slope is predictable from the EHP, the STR, or the TPM; the arguments have been developed for carbonyl addition reactions by Jencks and Cordes³² and the relations experimentally confirmed by do Amaral, Sandstrom, and Cordes.³³ According to the EHP or the TPM, electron withdrawal in R (larger σ_R) should lengthen N \cdots Si, leading to smaller S_R . An increase in n_N should also lengthen

(26) (a) G. S. Hammond, *J. Am. Chem. Soc.*, **77**, 334 (1955); (b) K. B. Wiberg, *Chem. Rev.*, **55**, 733, 737 (1955); (c) A. Streitwieser, Jr., *ibid.*, **56**, 571 (1956).

(27) C. G. Swain and E. R. Thornton, *J. Am. Chem. Soc.*, **84**, 817 (1962).

(28) (a) E. R. Thornton, *ibid.*, **89**, 2915 (1967).

(29) Good evidence for such conjugation exists: (a) C. Eaborn, "Organosilicon Compounds," Butterworth & Co. (Publishers) Ltd., London, 1960, p 94 ff; (b) R. West, L. S. Watley, and K. J. Lake, *J. Am. Chem. Soc.*, **83**, 761 (1961).

(30) C. G. Swain and C. B. Scott, *ibid.*, **75**, 141 (1953).

(31) S. I. Miller, *ibid.*, **81**, 101 (1959).

(32) Reviewed by W. P. Jencks, *Progr. Phys. Org. Chem.*, **2**, 63 (1964).

(33) L. do Amaral, W. A. Sandstrom, and E. H. Cordes, *J. Am. Chem. Soc.*, **88**, 2225 (1966).

N \cdots Si, giving a more negative ρ_N . Thus C should be negative by both arguments. The STR predicts that electron withdrawal in R will shorten N \cdots Si, increasing S_R (positive C), but also predicts that an increase in n_N will lengthen N \cdots Si, giving a more negative ρ_N (negative C). We therefore defer to the predictions of the EHP and the TPM in this case.³⁴

Role of $d\pi$ – $p\pi$ Bonding and Its Implications. A plot of Jaffé's values³⁵ for the (3d,2p)– π overlap integral as a function of internuclear distance reveals a sharp fall-off beyond the reactant Si–O distance³⁶ of 1.63 Å. It may well be, therefore, that if substitution in the aryl group induces changes in the activated complex Si–O distance, concomitant variations in $d\pi$ – $p\pi$ bonding may occur. Such a model can, in fact, account for the shape of the free energy curve of Figure 1.

Assume that the free-energy curve excluding π -bonding effects has the linear form of the dashed line in Figure 2. This is reasonable since the slope is intermediate between the extremes of $m \sim 0$ and $m \sim 1.2$ for the curves of Figure 1, as would be expected for an activated complex with a partially broken Si–OAr bond. Further assume that, with good leaving groups, the activated complex Si–OAr bond is sufficiently short that π bonding is still important, but that as the leaving group becomes worse and the bond lengthens, this bonding is lost. This would produce the deviation shown by the solid line on the right side of Figure 2, with good leaving groups being unusually good but with the π -bonding effect being gradually lost until the two curves finally intersect at the point where π bonding is unimportant in the activated complex. As the Si–OAr bond is lengthened, however, the CH₃O–Si bond is simultaneously shortened. At some point, it should become short enough that π bonding enters the picture for this bond and the deviation shown at the left of Figure 2 will now result. Thus variations in $d\pi$ – $p\pi$ bonding in the activated complex can account for the observed curvature in the free energy relations.

If this postulate is reasonable, similar observations should be made in other, related systems. Actually, the data of Åkerman¹⁸ for aryloxysilane solvolysis in aqueous ethanol show an exactly comparable curvature. So do the data of Eaborn and Walton³⁷ for cleavage of (C₂H₅)₃SiC \equiv CAr in methanol–water. On the other hand, no curvature appears in Hammett plots for cleavage of substituted benzyl groups from silicon,³⁸ a happy result since no π interactions are expected in this case of a saturated-carbon leaving group.

Furthermore, the phenomenon should also appear in leaving group reactivities from other second-row centers such as phosphorus. The results are: (a) for ROPO₃²⁻, the free energies of activation are a good linear function³⁹ of leaving group pK_a ; (b) for ROPO₃H⁻, there is concave-downward curvature³⁹ so that good leaving groups are less reactive than pre-

(34) The apparent experimental support for the STR prediction for carbonyl addition (L. B. Jones and T. M. Sloane, *Tetrahedron Letters*, 831 (1966)) can be understood if the entropy of the activated complex does not decrease monotonically with a decrease in the nucleophile–carbonyl distance. This now seems probable.²³

(35) H. H. Jaffé, *J. Chem. Phys.*, **21**, 259 (1953).

(36) Reference 29a, p 492.

(37) C. Eaborn and D. M. R. Walton, *J. Organometal. Chem.* (Amsterdam), **4**, 217 (1965).

(38) C. Eaborn and S. H. Parker, *J. Chem. Soc.*, 126 (1955).

(39) A. J. Kirby and A. G. Varvoglis, *J. Am. Chem. Soc.*, **89**, 415 (1967), and other papers cited there.

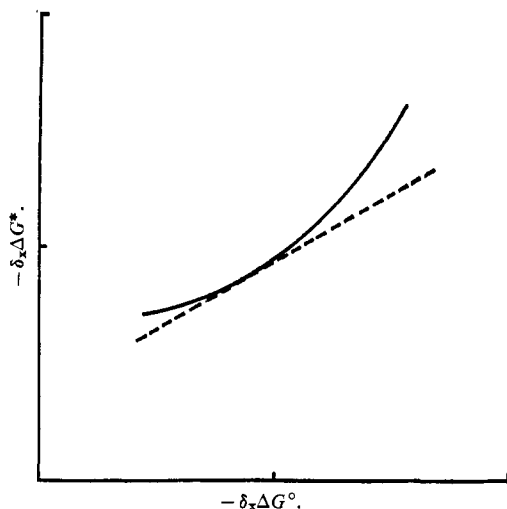


Figure 2. Hypothetical linear free energy relation for aryloxy-silane methanolysis (dashed line) modified by changes in π bonding of Si to leaving group (deviation on right-hand side) and entering group (deviation on left-hand side). Compare the solid line with Figure 1.

dicted; (c) for $\text{CH}_3\text{PO}(\text{OC}(\text{CH}_3)_2\text{H})\text{OAr}$, the reactivities for various Ar are given⁴⁰ as $p\text{-NO}_2\text{C}_6\text{H}_4 > p\text{-ClC}_6\text{H}_4 > \text{C}_6\text{H}_5 \approx \text{CH}_3\text{OC}_6\text{H}_4$. Result c for the phosphonate diester is in good accord with our hypothesis. Result a can be rationalized by assuming the phosphorus 3d orbitals to be saturated by the three O^- substituents so that π bonding to RO is not important. Result b is explained by Kirby and Varvoglis as being due to a change in mechanism with leaving group from rate-determining decomposition of $-\text{O}_3\text{P}^+(\text{OHR})$ to its rate-determining formation. This may well mask the π -bonding effect. We conclude that the data for phosphorus compounds are not in disagreement with the π -bonding hypothesis.

Conclusion

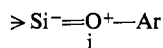
The isotope effect and substituent effect data for methanolysis of aryloxysilanes are in accord with a general base catalyzed process of the "solvation rule" class in which the leaving group substituent effect varies with leaving group from practically nil ($m \sim 0$) to very large values ($m \sim 1.2$). The latter phenomenon may result from either (i) a change in mechanism from an "Si-5" process⁴¹ to an SN_2 process or (ii) variations in Si-O $d\pi-p\pi$ bonding in the activated complex.

Although the data do not decide conclusively between these possibilities, we favor ii as more consistent with the limiting values of m found from Figure 1. If i were correct, we would expect a larger effect than $m \sim 0$ for formation of the Si-5 species, by analogy with carbonyl addition^{16,17} where the corresponding slope is 0.6. We would also expect a smaller value than 1.2 for the SN_2 mechanism, since the ArO bond should not be very completely broken, as argued above.⁴²

(40) Data of J. Epstein, cited by J. O. Edwards, "Inorganic Reaction Mechanisms," W. A. Benjamin, Inc., New York, N. Y., 1964, p 63.

(41) Or an "SN2*-Si-5" process: see ref 22 and also L. H. Sommer, G. A. Parker, N. C. Lloyd, C. L. Frye, and K. W. Michael, *J. Am. Chem. Soc.*, **89**, 857 (1967).

(42) A value larger than unity is conceivable, however, because of contribution of structures such as i to the reactant hybrid.



On the other hand, practically any limiting slopes could result from ii, including an inversion to a negative slope with sufficiently electron-donating substituents.

Experimental Section

Materials. Anhydrous sodium acetate (Fisher Certified), lithium perchlorate (G. Frederick Smith), and lithium chloride (Fisher Certified) were dried at 105° for 48 hr and stored over silica gel. Sodium methoxide solutions were prepared by dissolving freshly cut sodium in methanol and were standardized against potassium acid phthalate (Baker and Adamson Primary Standard).

Phenoxytriphenylsilane, *p*-chlorophenoxytriphenylsilane, *p*-methoxyphenoxytriphenylsilane, and (*p*-methylphenoxy)triphenylsilane were synthesized using the method described by Larsson⁴³ in which ethanol is distilled from a refluxing mixture of ethoxytriphenylsilane, the appropriate phenol, and a small piece of sodium. Fractional vacuum distillation of the resulting dark brown solid, followed by recrystallization from petroleum ether (bp $30\text{--}70^\circ$), gave the desired silane.

(*m*-Trifluoromethylphenoxy)triphenylsilane was prepared from chlorotriphenylsilane and the appropriate phenol with pyridine acting as a hydrogen chloride acceptor, following a procedure similar to that of Gerrard and Kilburn.⁴⁴ To obtain the *m*-trifluoromethylsilane, 0.1 mole of chlorotriphenylsilane (Peninsular Chemical Co.) dissolved in petroleum ether (bp $60\text{--}110^\circ$) was added dropwise to a solution of 0.1 mole of *m*-trifluoromethylphenol (Pierce Chemical Co.) and 0.1 mole of pyridine (Fisher reagent grade) in petroleum ether (bp $60\text{--}110^\circ$). After refluxing the solution for 2 hr, the pyridine hydrochloride was filtered off and the solvent removed. Fractional vacuum distillation followed by recrystallization from petroleum ether (bp $30\text{--}60^\circ$) gave the silane in 86% yield, mp $60.5\text{--}61.0^\circ$.

Methanol-*d*. CH_3OD was synthesized from dimethyl carbonate (Eastman White Label), deuterium oxide (Bio-Rad), and dimethyl sulfate catalyst (Mallinckrodt OR), following the procedure described by Streitwieser, Verbit, and Stang.⁴⁵ The final distillation from sodium was performed as the methanol-*d* was needed. Vapor phase chromatography using a Carbowax 20M column indicated no impurities in the final product.

Kinetic Measurements and Data Treatment. Absorption measurements were made on either a Cary Model 14 spectrophotometer or a Beckman DB spectrophotometer with attached log potentiometric recorder. The latter instrument was also equipped with a constant-temperature cell block which was used when samples had to be left in the instrument for a sustained length of time. A matched set of four glass-stoppered Pyrocell silica cells were used in obtaining the absorption readings. Constant temperature was maintained by use of a thermostatically controlled water bath in which flasks could be immersed. A recirculating pump was used to maintain a flow of water through the spectrophotometer constant-temperature block. Temperatures were maintained within 0.1° of the stated value.

Observed first-order rate constants were calculated by means of the integrated form of the first-order kinetic rate law, using a least-squares method and the IBM 7040 computer.

Kinetic Procedures. Wavelengths ($m\mu$) used for following the kinetic progress of each reaction were (substrate, method A, method B): *p*- $\text{CH}_3\text{OC}_6\text{H}_4\text{OSi}(\text{C}_6\text{H}_5)_3$, 390, 286.5; *p*- $\text{CH}_3\text{C}_6\text{H}_4\text{OSi}(\text{C}_6\text{H}_5)_3$, 280, 283.0; $\text{C}_6\text{H}_5\text{OSi}(\text{C}_6\text{H}_5)_3$, 271.8, 266.0; *p*- $\text{ClC}_6\text{H}_4\text{OSi}(\text{C}_6\text{H}_5)_3$, 284.0, 277.0; *m*- $\text{CF}_3\text{C}_6\text{H}_4\text{OSi}(\text{C}_6\text{H}_5)_3$, 285.0, —.

A. Acetate Buffers. Methanolysis reaction rates were determined by spectrophotometrically following the increase in ultraviolet absorption due to formation of the phenol product. The aryloxy-silane reactant was dissolved in the acetate buffer of desired strength, using a glass-stoppered volumetric flask; this flask was thermostated at 27.4° and samples were withdrawn periodically for ultraviolet absorption analysis. In the cases of the *m*-trifluoromethyl reactant and of solvolysis in CH_3OD , this procedure was modified by transferring a sample of the reaction solution to the stoppered ultraviolet cell, which was inserted into the constant-temperature block of the Beckman spectrophotometer; absorption readings were then made on a continuous basis.

B. Phenoxide Buffers. Determination of the methanolysis reaction rates was made by spectrophotometrically measuring the

(43) E. Larsson, *Chem. Ber.*, **86**, 1382 (1953).

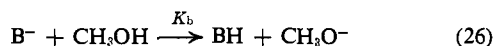
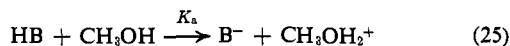
(44) W. Gerrard and K. D. Kilburn, *J. Chem. Soc.*, 1536 (1956).

(45) A. Streitwieser, Jr., L. Verbit, and P. Stang, *J. Org. Chem.*, **29**, 3706 (1964).

decrease in aryloxysilane concentration after simultaneously quenching the reaction and removing the phenoxide buffer by means of an extraction technique.

Stock solutions of reactant silane dissolved in 0.1500 M LiClO₄ in methanol solution and of phenoxide buffer were thermostated at 27.4°; both of these solutions were double the concentration desired in the reaction solution. Five milliliters of each solution was rapidly mixed in a 50-ml flask, and after the desired interval of time the reaction was quenched in an extraction solution of 10 ml of cyclohexane (practical grade) and 10 ml of aqueous sodium hydroxide, sufficiently basic to neutralize all the phenol present. After separation of the two phases, the cyclohexane solution was further extracted with 10 ml of dilute aqueous HCl and with 5 ml of distilled water, dried with anhydrous sodium sulfate, and subjected to the absorbance analysis. Control experiments showed the silane-phenol buffer separation to be quantitative; rate constants using this procedure were obtained for the *p*-chlorosilane reactant in acetate buffer and were identical with those obtained using method A.

Acid-Base Equilibria in Methanol. The dissociation constants K_a and K_b as defined by eq 25 and 26 were derived for acetic acid,



phenol, and *m*-trifluoromethylphenol in methanol solvent. These measurements were carried out at 27.4° and an ionic strength of 0.1500 M so as to duplicate the environment in which the methanolysis reactions were conducted. The results obtained using the methods described below are tabulated in Table IV.

Table IV.^a Equilibrium Constants in Methanol at 27.4 ± 0.1° ($\mu = 0.1500 M$)^b

HA	pK_b	pK_a
CH ₃ CO ₂ H	7.48	9.44
C ₆ H ₅ OH	2.66	14.26
<i>m</i> -CF ₃ C ₆ H ₄ OH	3.76	13.16

^a pK_b determined experimentally; pK_a calculated from $pK_{\text{auto}}(\text{CH}_3\text{OH}) = 16.92$ (E. Grunwald and E. Price, *J. Am. Chem. Soc.*, **86**, 4517 (1964)). ^b Maintained by added LiClO₄.

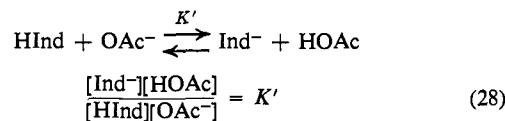
K_b of Phenol. A series of phenol-phenoxide buffers was prepared from phenol and sodium methoxide solution with [added phenol] $\approx 4 \times 10^{-4} M$ and [added methoxide] varying between 0.01 and 0.04 M. The absorbance A of each buffer was measured at 288 m μ , a wavelength at which phenoxide ion is the only absorbing species. These data were fitted to eq 27, derived by Stearns

$$\frac{[\text{added phenol}]}{A} = \frac{1}{k''} + \frac{K_b}{k''} \frac{1}{[\text{MeO}^-]} \quad (27)$$

and Wheland,⁴⁶ using a least-squares plot of $1/[\text{MeO}^-]$ vs. [added phenol]/ A ; from the slope K_b/k'' and intercept $1/k''$, K_b can be determined. $[\text{MeO}^-]$, however, is not accurately known because of phenoxide solvolysis, so $[\text{MeO}^-]$ was redetermined using the calculated K_b value and a new plot was made. This iteration procedure was continued, using an IBM 7040 computer, until K_b remained constant on successive calculations ($|(K_2 - K_1)/K_2| < 0.0001$).

K_b of *m*-Trifluoromethylphenol. The same mathematical procedure described above was used for this determination. The buffer solution had [added *m*-trifluoromethylphenol] = $2.37 \times 10^{-4} M$ and [added methoxide] = $(2-8) \times 10^{-4} M$; the wavelength used was 300 m μ . Before preparing the buffer solutions, the *m*-trifluoromethylphenol (Pierce Chemical Co.) was purified by vacuum distillation since the reagent grade chemical was unavailable.

K_b of Acetic Acid. The method used in this determination was calculation of K_b for an indicator, in this case bromocresol green (BCG), and utilization of this value in conjunction with acetate buffers containing BCG indicator. K_b of acetic acid was derived by use of eq 28 and 29.



$$pK_b(\text{HOAc}) = pK_b(\text{HInd}) + pK' \quad (29)$$

A stock indicator solution was prepared by dissolving in methanol a weighed sample of the disodium salt of BCG (Matheson Coleman and Bell), previously dried at 105°; using added sodium methoxide to ensure complete conversion to the basic form (Ind⁻), a molar extinction coefficient ϵ of 3.81×10^4 was determined at 617 m μ , a wavelength at which the acidic form (HInd) does not absorb. K_b for BCG was calculated using the observed absorbance A at 617 m μ assuming that $[\text{HInd}] = [\text{MeO}^-]$. A value of $K_b(\text{BCG}) = 1.70 \times 10^{-8}$ ($pK_b = 7.770$) was obtained.

Three acetic acid-acetate buffers containing known [added BCG] were prepared and their absorbance was measured at 617 m μ . An average K' value of 1.932 ± 0.015 ($pK' = -0.286 \pm 0.003$) was derived, leading to a pK_b value of 7.484 for acetic acid.

K_b of Acetic Acid in Methanol-*d*₁. The procedure described in the preceding section was repeated using methanol-*d*₁ as the solvent. The various calculated constants in the medium are: $\epsilon = 3.911 \times 10^4$; $K' = 1.856$; $pK' = -0.269$; $K_b(\text{BCG}) = 2937 \times 10^{-8}$; $pK_b(\text{BCG}) = 7.532$; $pK_b(\text{HOAc}) = 7.263$.

(46) R. S. Stearns and G. W. Wheland, *J. Am. Chem. Soc.*, **69**, 2025 (1947).